In vivo localised gastrocnemius subtendon representation within the healthy and ruptured human Achilles tendon

Ra'ad M. Khair [1*], Lauri Stenroth [2], Neil J. Cronin [1,4], Aleksi Reito [3], Juha Paloneva [3] and Taija Finni [1].

[1] Faculty of Sport and Health Sciences, Neuromuscular Research Center, University of Jyväskylä, Jyväskylä, Finland; [2] Department of Applied Physics, University of Eastern Finland, Kuopio, Finland; [3] Central Finland Health Care District, Finland and University of Eastern Finland, Finland, [4] School of Sport and Exercise, University of Gloucestershire, UK.

*Author for Correspondence

Ra'ad M. Khair

Email: raad.m.khair@jyu.fi

Phone : +358469221362

P.O. Box 35

40014 Jyväskylä, Finland

Author contributions

Conceptualization: T.F., N.J.C., A.R., J.P., R.M.K; Methodology: T.F., N.J.C., A.R., L.S., J.P.; Data acquisition: T.F., R.M.K.; Data curation - analysis: R.M.K.; Writing original draft: R.M.K.; Writing – review & editing: R.M.K., L.S., N.J.C., A.R., J.P., T.F.; Visualization: R.M.K.; Supervision: T.F., N.J.C.; Funding acquisition: T.F; Project administration: T.F.

Abstract

The Achilles tendon (AT) is composed of three distinct in-series elastic subtendons, arising from different muscles in the triceps surae. Independent activation of any of these muscles is thought to induce sliding between the adjacent AT subtendons. We aimed to investigate displacement patterns during voluntary contraction (VOL) and selective transcutaneous stimulation of medial (MG_{stim}) and lateral (LG_{stim}) gastrocnemius between ruptured and healthy tendons, and to examine the representative areas of AT subtendons. Twenty-eight patients with unilateral AT rupture performed bilateral VOL at 30% of the maximal isometric un-injured plantarflexion torque. AT displacement was analysed from sagittal B-mode ultrasonography images during VOL, MG_{stim} and LG_{stim}. Three-way ANOVA revealed a significant two-way interaction of contraction type*location on the tendon displacement ($F(10\text{-}815)=3.72$, $p<0.001$). The subsequent two-way analysis revealed a significant contraction type*location interaction for tendon displacement ($F(10\text{-}410)=3.79$, $p<0.001$) in the un-injured limb only, where LG_{stim} displacement pattern was significantly different from MG_{stim} ($p=0.008$) and VOL ($p=0.005$). When comparing contraction types between limbs the there were no difference in the displacement patterns, but displacement amplitudes differed. There was no significant difference in the location of maximum or minimum displacement between limbs. The displacement pattern was not different in non-surgically treated compared to un-injured tendons one-year post rupture. Our results suggest that near the calcaneus, LG subtendon is located in the most anterior region adjacent to medial gastrocnemius. However, free tendon stiffness seems to be lower in the injured AT, leading to more displacement during electrically-induced contractions compared to the un-injured.

New & Noteworthy

Using selective electrical stimulation, we report the distributions of medial and lateral gastrocnemius subtendon representations within the healthy and ruptured Achilles tendon. In the majority of our sample, lateral gastrocnemius subtendon was found in the most anterior region adjacent to medial gastrocnemius both in the healthy and ruptured, non-surgically treated tendon. The tendon internal displacement pattern does not seem to differ, but displacement amplitude and non-uniformity differed between healthy and ruptured tendons one-year post rupture.

Key words: Achilles tendon, architecture, geometry, anatomy, rupture, human.

Introduction

The Achilles tendon (AT) provides critical series elasticity to the triceps surae, amplifying power for activities such as walking and running (1) and playing a significant role in mechanical energy storage (2). Normal tendon function is disrupted by AT disorders that also cause pain and disability. Achilles tendon rupture (ATR) is prevalent in sport-related activities with an incidence of 31/100,000 individuals per year (3, 4). Understanding the normal and pathological biomechanical function of the AT is crucial to the diagnosis and management of AT-related maladies.

The AT has a complex hierarchical structure and is composed of distinct bundles of fascicles running continuously along the tendon, called subtendons. AT subtendons each arises from a different muscular head of the triceps surae: soleus (SOL), medial gastrocnemius (MG), and lateral gastrocnemius (LG) (5, 6). The tendon twists so that at the calcaneal tuberosity insertion, the MG fibres are located on the lateral surface, LG fibres more deeply, and the SOL fibres on the medial surface (5, 6). The degree of twist varies among individuals and can be classified into three types (5). This variation might lead to interindividual differences in the location of the MG, LG and SOL tendon fascicles along the length of the tendon (5). Due to this structure, AT is subjected to complex non-uniform loading that can cause heterogeneity of strain within the tendon (7).

In vivo studies have exploited advances in ultrasonic imaging and speckle tracking algorithms to reveal non-uniform motion within the AT (8, 9). The ability of subtendons to slide relative to each other is considered to be a function of a healthy tendon (9, 10). Healthy non-uniformity is characterised by smaller displacement of the superficial (posterior) tendon and larger displacement of the deep (anterior) tendon. Assuming that posteriorly the tendon consists of fascicles arising from both gastrocnemius muscles and that the anterior tendon consists of fascicles arising from soleus, researchers have tried to identify structure-function relationships

(11, 12). However, the mechanism of non-uniform displacement and the representation of each subtendon within free AT in different individuals remains elusive due to potential differences in neural control strategies (7), the architecturally complex twisted tendon structure (5, 6), and the difficulty of visualizing individual subtendons using conventional imaging techniques (ultrasound or magnetic resonance imaging).

In recent studies, ruptured ATs have been found to display more uniform within-tendon displacement 1-year post-rupture (13, 14). In addition to an increase in length of the tendon, ATR leads to morphomecahnical changes in the triceps surae muscles and subtendons (15, 16). These changes seem to occur regardless of whether they were treated surgically or conservatively (13, 14), and might alter the force transmission mechanism in the muscle-tendon unit.

Voluntary contraction typically activates all synergistic muscles to a variable degree (17, 18) and leads to disproportionate tissue displacement within the tendon due to mechanical and structural differences between triceps surae muscles (19). During voluntary contractions, complex neuromuscular control of the triceps surae within and across healthy and injured individuals may confound interpretations of tissue displacement in adjacent subtendons. By removing the effects of neural control, one could potentially identify if changes in structure and material properties due to ATR modify the displacement pattern within the AT. Electrical transcutaneous stimulation can be used to stimulate a given muscle selectively (20, 21). Using this method, it can be assumed that selective activation of one of the triceps surae muscles induces serial force transmission that is observed as tendon displacement mainly in the area containing tendon fascicles arising from the activated muscle belly. Therefore, the stimulation method may also help to understand AT subtendon organization in vivo.

By using selective transcutaneous stimulation to medial and lateral gastrocnemius muscles we aimed to find out whether AT tissue displacement pattern differs in voluntary contraction and

electrically evoked contractions between injured (INJ) and un-injured (UNJ) tendons. Examination of the displacement patterns during selective activation was expected to yield information about the representative areas of AT subtendons. We hypothesized that different contraction types would lead to different displacement patterns. Furthermore, it was hypothesized that INJ tendon would show less, and more uniform displacement compared to the UNJ tendon.

Methods

Participants

Twenty-eight ATR patients (24 males, 4 females) treated at the Central Finland Health Care District agreed to participate (Table 1). ATR was diagnosed according to the American Academy of Orthopaedic Surgeons guidelines. Inclusion criteria were a minimum of 2 of the following 4 criteria: a positive Thompson test, decreased plantarflexion strength, presence of a palpable gap, and increased passive ankle dorsiflexion with gentle manipulation. Participants with re-occurring rupture were treated surgically and excluded from the sample, which contains only individuals with non-surgical treatment and early mobilization (22). This study was approved by the Ethics committee of Central Finland health care district (2U/2018). Participants signed an informed consent explaining the details of the study, possible risks, and gave permission to use data for research purposes. Participants were invited to the laboratory 1-year ± 1.8 months after rupture.

Table 1. Patient characteristics, free Achilles tendon length, and medial and lateral gastrocnemius subtendon lengths (mean ± SD).

Participants (N=28)		
Age (years)	42.4 ± 9.3	
Height (m)	1.76 ± 0.08	
Body mass (Kg)	82.5 ± 12.2	
Limb condition	**Un-injured**	**Injured**
Free tendon length (cm)	8.79 ± 3.47	10.36 ± 3.71
MG subtendon length (cm)	18.90 ± 1.92	20.99 ±2.20
LG subtendon length (cm)	21.59 ± 1.60	23.51 ± 1.99

Experimental procedure

B-mode ultrasound was used to examine tendon properties. Scans were done using a 3.6-cm linear probe (UST-5411, Aloka alpha10, Japan). First, the subtendon lengths of MG, LG and SOL were measured from a resting prone position with the subjects' feet over the edge of a table. The limb was scanned to find the most distal point of the muscle-tendon junction of each muscle head and the tendon insertion on the calcaneus, all of which were marked on the skin. The distance between the points was then measured with a measuring tape (23). The reliability of this method was tested, whereby four un-injured limbs was measured on two separate days. The subtendon lengths of the triceps surae muscles were measured and the intraclass correlation coefficient (ICC) was calculated (24). ICC was 0.99 (90% CI 0.97- 0.99) with a coefficient of variation (CV) of 6.6%. Ultrasound imaging was then used to locate the thickest part of both gastrocnemius muscles, where the stimulating electrodes were placed. Participants´ skin was shaved and cleaned with alcohol to ensure good conductivity. A pair of 32 mm diameter electrodes (Niva Medical Oy) was attached over each muscle with ~1 cm inter-electrode distance. During measurements, participants sat in a custom-made ankle dynamometer (University of Jyväskylä, Finland) with the hip at 120°, knee at 0° (fully extended), and the ankle and first metatarsophalangeal joints at 90° and 0° respectively. The foot was strapped to the dynamometer pedal and the thigh secured to the seat above the knee. To image tendon displacement, the ultrasound probe was attached longitudinally with the distal edge ~2 cm above the calcaneus.

A warm-up was done in the form of a series of standardized submaximal contractions. Starting with UNJ, unilateral maximal voluntary isometric contractions (MVCs) were performed followed by contractions corresponding to 30% of UNJ MVC. Then, with the participant relaxed, single stimulation pulses were elicited with increasing intensity using a constant

current electrical stimulator (DS7AH; Digitimer, Hertfordshire, UK) until the motor threshold was exceeded, as confirmed by a visible muscle twitch (20, 21). If a corresponding displacement was not observed clearly in the US image of the AT, higher stimulation intensity was used. AT displacement was imaged 1 s before and throughout a tetanic pulse of 1000 μs at 100 Hz at the pre-determined stimulation intensity. MG and LG were stimulated in random order. The entire protocol was then repeated for INJ, starting with voluntary isometric contractions, followed by electrically induced contractions.

Force data were collected via a strain gauge transducer in the foot pedal of the ankle dynamometer. A potentiometer placed under the heel was used to detect heel lift during contractions. Data were sampled at 1 kHz via a 16-bit A/D board (Power 1401, Cambridge Electronic Design, Cambridge, UK) connected to the computer, and signals were recorded using Spike2 software (Cambridge Electronic Design, Cambridge, UK). To synchronize data, a TTL-pulse was sent manually via Spike2 to first trigger the data acquisition with the US device for 8 seconds and after 1 s to deliver the 0.7 s tetanus to either MG or LG. Ultrasound videos were sampled at 50 HZ and stored for further offline analysis.

Data analysis

Ultrasound B-mode image analysis of tendon displacement was done using a speckle tracking algorithm implemented in Matlab (R2020a, MathWorks Inc, Natick, MA, USA) according to the previously validated and published configuration of Slane and Thelen (9, 25). The region of interest location and size were defined for each subject manually to ensure that only tendon tissue was analysed. A grid of six nodes across the width of the tendon and eleven across the length of the tendon was generated (14). All tracking results were visually inspected to ensure that the nodes remained inside the tendon throughout the movement. Incremental displacements were fitted with a low-order polynomial (25). Displacements of nodes along each of the six antero-posterior rows were averaged and peak displacement of the average data

were extracted for analysis. The six locations across the tendon starting from the posterior part to the anterior part are referred to as locations 1-6, respectively. The average peak displacement across the six locations was used to represent mean displacement. Locations of the maximum and minimum displacement were extracted. Tendon non-uniformity was expressed as the difference between minimal and maximal displacement in the tendon. To facilitate the comparison of displacement patterns between electrically induced contractions and volitional activation, the displacement data were normalized to a range between 0-1 where 0 is minimum displacement location and 1 is maximum displacement location. The relative displacement relation between 6 locations across the tendon is hereafter referred to as the displacement pattern. Displacement was normalized since voluntary contraction produced higher torque and overall AT displacement than electrically induced contractions. Peak torque was calculated for both voluntary and electrically induced contractions.

Statistical analysis

Statistical analysis was performed using JASP (JASP version 0.14.1, Amsterdam, Netherlands). The level of significance was set at $p<0.05$. Three-way repeated-measures ANOVA was performed to investigate the effects of contraction type (VOL, MG, and LG stimulations), limb condition (INJ vs UNJ) and tendon location (across 6 locations) on the normalized displacement of the tendon. The main interest of the analysis is in three- and two-way interaction effects, indicating how the displacements are distributed between the tendon locations (i.e. are affecting the displacement pattern) in the different conditions and limbs. If significant three-way interactions were detected, two-way analysis was performed, followed by simple pairwise comparisons with Bonferroni-adjustment when a significant main effect was found. Greenhouse-Geisser adjustment was applied when the assumption of sphericity was violated. Skewness and kurtosis was checked to insure the normality of the data. If outliers

where detected, the test was done with (i.e. the entire sample) and without the outlier. Limb differences (UNJ vs INJ) in AT non-uniformity, displacement amplitude, maximum and minimum displacement locations were compared using two-sided paired t-tests.

Results

Free tendon length below the SOL muscle insertion site was significantly longer in INJ compared to UNJ with a mean difference (95%CI) of 1.6 cm (0.6-2.6 cm; p=0.003). The INJ MG subtendon was also longer by 2.1 cm (1.5–2.7 cm; p<0.01), and LG by 1.9 cm (1.2–2.6 cm; p<0.01) than in UNJ. There were no statistically significant differences in stimulation threshold or intensity between limb muscles or between limbs (Table 2).

Table 2. Descriptive data of motor thresholds, selective electrical stimulation-induced contractions intensities of medial (MG) and lateral (LG) gastrocnemius muscles in the un-injured and injured limbs, and comparisons between limbs and muscles.

	Injured		**Un-injured**		***P*-values comparing stimulations**			
	MG	**LG**	**MG**	**LG**	between limbs		between muscles	
					MG	**LG**	**INJ**	**UNJ**
Stimulation intensity mA (SD)	20.36 (9.26)	18.48 (5.63)	17.75 (9.26)	16.07 (7.37)	0.164	0.155	0.413	0.097
Threshold mA (SD)	15.50 (9.75)	15.25 (4.76)	14.07 (7.98)	19.75 (7.71)	0.513	0.408	0.634	0.210

P-values using un-adjusted pairwise t-test.

Absolute displacement values and torque levels are reported in (Table 3). There was no statistically significant difference in stimulation evoked torque levels between limbs in response to stimulation of either muscle despite the stimulation inducing a significantly higher mean displacement in both INJ in muscles compared to UNJ. The mean (SD) magnitude of

heel lift during electrically induced contractions was 0.04 mm (0.5) and 2.5 mm (4.0) during voluntary contractions.

Table 3. Descriptive data of mean displacement, non-uniformity, and absolute torque of electrically induced and voluntary contractions.

	Injured			**Un-injured**		
	MG	**LG**	**VOL**	**MG**	**LG**	**VOL**
Mean displacement mm (SD)	0.93 (0.65)	0.65 (0.57)	3.52 (1.71)	0.61 (0.48)	0.39 (0.27)	3.63 (1.18)
Tendon non-uniformity mm (SD)	0.14 (0.11)	0.15 (0.12)	0.85 (0.79)	0.25 (0.23)	0.24 (0.17)	1.48 (1.04)
Torque Nm (SD)	5.18 (2.98)	3.24 (2.72)	57.98 (16.30)	5.56 (4.05)	3.67 (2.53)	57.78 (16.23)

Voluntary and stimulation-induced displacement patterns

To explore the differences in displacement patterns, the absolute values of the 6 locations were normalized to enable comparison between VOL and stimulation conditions (Figure 1). Three-way repeated-measures ANOVA was performed to evaluate the effects of contraction type, location and limb condition on tendon displacement. There was a significant two-way interaction of contraction type*location on the tendon displacement ($F_{(10\text{-}978)} = 3.7$, $p<0.001$). Initial three-way analysis was followed by a two-way repeated-measures ANOVA for the effect of contraction type*location on tendon displacement at the two levels of limb

condition and the location*limb condition on tendon displacement at each contraction type level.

There was no significant location*limb condition interaction effect on tendon displacement at each contraction type level. There was a significant contraction type*location interaction effect on tendon displacement ($F(10\text{-}492) = 3.8$, $p<0.001$) at the UNJ limb, while the interaction effect was not significant for the INJ limb ($F(10\text{-}486) = 1.11$, $p=0.353$). Simple pairwise comparisons were done between the contraction types for the UNJ with a Bonferroni adjustment applied. The analysis showed that the LG_{stim} displacement pattern was significantly different to MG_{stim} ($p=0.007$), and VOL ($p=0.003$) (Figure 1). Individual displacement patterns are shown in (Figure 2).

In UNJ, maximum displacement during MG_{stim} occurred most frequently in the three most anterior locations, while during $LG_{stim,}$ maximum displacement occurred most often in the most anterior (6^{th}) location (Figure 4). This pattern was also found in INJ, where the most frequent locations of maximum displacement during MG_{stim} were in the anterior half of the tendon (frequency of maximal displacement: 4^{th}: 21.4%, 5^{th}: 32.2% and 6^{th}: 32.7%), while during $LG_{stim,}$ maximum displacement occurred in the 6^{th} location in 48.2% of participants. Minimum displacement was found in the most posterior location for the stimulation of both muscles in both limbs. There was no statistically significant difference in maximum or minimum displacement location between limbs.

Tendon non-uniformity and displacement amplitude during electrical stimulation

Tendon non-uniformity was higher in UNJ compared with INJ with a mean difference (95%CI) of 0.11 mm (0.04 – 0.18mm, $p=0.005$) during MG_{stim}, and 0.09 mm (0.03 – 1.42 mm, $p<0.001$) during LG_{stim} (Figure 3). When non-uniformity was compared between stimulated muscles in

the same limb, there was no statistically significant difference in either limb, with a mean difference (95%CI) of 0.016 mm (-0.06 – 0.09 mm) for UNJ and 0.003 mm (-0.05 – 0.05 mm) for INJ. One outlier was detected in LG_{stim} mean displacement group (Higher range:1.9mm, outlier:2.7mm), when the whole sample was used there was no significant difference in mean tendon displacement of the INJ between the contractions induced when stimulating different muscles, with a mean difference (95%CI) of 0.28 mm (-0.004 – 0.56 mm, p=0.053), however when the test was done without the outlier there was a significant difference (95%CI) of mean difference of 0.34 mm (0.007 – 0.61 mm, p=0.015). In the UNJ, there was a significant difference in the mean displacement depending on the stimulated muscle, with a greater displacement when MG was stimulated (95%CI) of mean difference of 0.22 mm (0.04 – 0.40 mm, p=0.016).

Discussion

In this study, we examined internal AT displacement patterns during voluntary and selective transcutaneous stimulation of medial and lateral gastrocnemius to investigate differences within the AT tissue displacement between INJ and UNJ limbs of patients after AT rupture and to inspect the representative areas of subtendons. The lowest stimulation intensity that induced a visible contraction was used to ensure selective activation of only the targeted muscle. As hypothesized, displacement patterns during voluntary and electrically induced contractions were different; the displacement pattern was significantly different during LG_{stim} compared to VOL and MG_{stim} in both limbs. There was no statistically significant difference when the displacement patterns were compared for each stimulated contraction between limbs. Thus, with the assumption that the stimulation-induced force is primarily serially transmitted to tendon fascicles, the subtendon organization does not seem to be altered in the non-surgically treated limb of ATR patients. In UNJ, peak tendon displacement during MG_{stim} tended to occur more posteriorly compared to VOL. Overall, the anterior half of the AT underwent larger displacement than the superficial posterior part in all contraction conditions.

Despite higher mean displacement in INJ, displacement was more uniform when compared to UNJ during contractions induced by stimulating MG and LG. Tendon stiffness also seemed to be lower in INJ, since ankle joint torque was similar during muscle stimulations in both limbs, but the displacement was larger in INJ than in UNJ. However, this was not observed for voluntary contractions in which tendon mean tendon displacement did not differ between the limbs. Marked inter-individual differences were observed in internal tendon motion. Thus, when investigating AT anatomical organization and internal force sharing, an individualized approach might help to understand AT force sharing mechanisms and tendon recovery from injury.

Voluntary vs. stimulated contractions

Internal tendon displacement patterns were different during LG_{stim} compared to VOL and MG_{tim} in UNJ. In VOL, peak displacement was typically found in the two most anterior locations. Voluntary contraction leads to disparate tissue displacement within the tendon due to disproportionate activation of synergistic muscles and mechanical structural differences between triceps surae muscles (7, 19). On the other hand, the low, stimulation-induced force can be assumed to be mainly transmitted serially to the targeted muscle's subtendon (26). Although lateral force transmission may occur (21), the main pathway of force is the stiffest structure. Hence, the location of peak displacement in response to stimulation can be considered to reveal the location of tendon fascicles within the cross-section of AT.

Displacement during LG_{stim} peaked in the anterior tendon, implying that the most anterior area could be occupied by tendon fascicles arising from LG subtendon. In anatomical studies, Pękala et al. (2017) and Edama et al. (2015) found that SOL occupied the anterior portion and LG the lateral portion of the tendon at the level of the SOL muscle-tendon junction. However, due to high torsion within AT, LG tendon fascicles are likely located anteriorly in the more distal tendon (5, 6). Furthermore, in a recent study, three tendons were dissected, and 3D computer aided models were constructed based on these tendons. In the model that twisted the most, LG subtendon was found to completely occupy the anterior portion of the distal AT (27). Therefore, anatomical studies are consistent with the present observations regarding the location of the LG subtendon.

There was no difference between VOL and MG_{stim} displacement patterns (Figure 1). However, during MG_{stim} displacement peaked around the 4th and 5th locations in UNJ, indicating that fascicles originating from MG could be present in the mid-to-anterior part of the tendon. Unlike in LG_{stim}, there was more individual variation in the location of peak displacement in MG_{stim}. Due to individual differences in free tendon length, the superior-inferior field of view may not

have been consistent across subjects relative to tendon length. When comparing these observations to the anatomical maps provided by previous cadavers studies, natural anatomical variation may explain the observed heterogeneity in peak displacement in response to MG_{stim} (5, 6, 27).

In addition to the anatomical origin, the observed peak displacement locations may have been affected by lateral force transmission between different subtendons within the AT. Each subtendon transmits the force from a single muscle belly but not fully independently, and force could be laterally transmitted between triceps surae muscle bellies or even subtendons (28, 29). AT force and subsequent displacement might be distributed unevenly with a bias toward the SOL subtendon since SOL subtendon fascicles have been found previously to be compliant in rats (29) and in human cadavers (30) although contradictory results have also been reported (27). This raises questions about the forces transmitted through connective tissue or inter-fascicular matrix, which could be crucial for force transmission mechanisms and inter-fascicular gliding within the tendon (10, 31).

In summary, during VOL and electrically induced contractions of MG and LG, minimum displacement always occurred in the posterior tendon and maximum displacement in the mid-to-anterior tendon. The same observation was made in a recent study where SOL and MG were electrically stimulated (32), and the tendon was split into two halves for analysis purposes; the anterior half always displaced the most in response to MG and SOL stimulations in different ankle positions. This is consistent with the observations made in this study as we found that the mid-to-deep part of the tendon displaced most when MG was stimulated and the deep part when LG was stimulated. The difference between the two studies is in the interpretation of the data in regard to which subtendon are presented in the deep part of the tendon. In Lehr et al. the tendon was split in consideration to the function-structure relationship (11, 12), and the authors interpreted a larger non-uniformity and displacement in the representative part of the

stimulated muscle tendon when SOL was stimulated compared to MG as an evidence of consistency with the anatomical function-structure consideration (32). We relied on the principle that the main pathway of force is the stiffest structure. Thus, when a muscle is selectively stimulated the arising regional tendon displacement can inform us about regions of the tendon corresponding to fascicles arising from different triceps surae muscles. Based on the beforementioned we found that the gastrocnemius subtendons are located in the mid-to-anterior part of the tendon, and that LG is probably located most anteriorly.

Gastrocnemius and soleus have different functional roles, despite having a common distal tendon and working synergistically as ankle plantar flexors (33, 34). It has been suggested that in order to perform their differing functional roles, these muscles rely on the ability of the subtendons to displace relative to each other (35, 36). It is of interest to investigate if normal subtendon organization can be restored after ATR as this most likely is a prerequisite for restoring normal Achilles tendon and triceps surae function including the functional independence of the muscles. If tendon fascicles that were originally part of different subtendons would merge during the healing process this could result in reduced capacity for relative movement between subtendons and disruption of the normal function of the Achilles tendon. In fact, ATR followed by surgical reconstruction has been shown to reduce non-uniform tendon motion observed using speckle tracking (8, 37). Our tendon displacement data (Figure 2) and our previous report (14) suggest that there are considerable individual variations in the subtendon organization in both ruptured and un-injured tendons. This signifies the importance of an individualized assessment and interpretation of the subtendon organization and function after ATR.

Tendon non-uniformity and displacement amplitude during electrical stimulation

Consistent with previous studies, we found a more uniform displacement pattern in INJ compared to the contralateral tendon 1-year post rupture (13, 14), suggesting impaired sliding within the injured tendon. Limited inter-fascicular sliding might be a result of interfascicular matrix adhesions caused by the rupture (10). Mean displacement in INJ was higher than in UNJ. As the same amount of torque was produced during stimulation, this result suggests lower stiffness in INJ. However, this differs from our previous results, where we reported that stiffness of the entire MG tendon during isometric voluntary contraction was similar between injured and un-injured tendons 1-year post rupture (38). This would suggest that in the free distal AT, mechanical properties (stiffness) may be altered locally and manifest themselves at low force levels, while globally stiffness seems to be similar between limbs. This discrepancy between our observations could indicate an extension of the toe region, or slackness of the tendon in the INJ limb while the linear region of the force-displacement curve would be similar between the limbs. A similar phenomenon of an extended range of tendon strain at low stresses has been reported previously after 4 weeks of limb unloading by suspension (39).

We found no differences between limbs (UNJ vs INJ) in the locations of maximum or minimum displacement when stimulating either MG or LG, consistent with our previous findings during voluntary contractions (14). Furthermore, in the three contraction types the displacement patterns were similar when compared between limbs. Thus, the anatomical subtendon organization does not seem to be altered after a rupture in non-surgically treated tendons.

Limitations

There are several limitations of this study. First, the nature of two-dimensional imaging may not fully capture the complex three-dimensional behaviour of the triceps surae subtendons,

which could lead to errors when estimating AT tissue displacement. The speckle tracking algorithm uses a low order polynomial fit to regularize displacement (25). This may reduce variation in displacement between the six locations across the tendon. However, filtering has been deemed necessary to reduce noise and erroneous estimates (40), and was applied here in the same manner as in previous studies (32). Furthermore, it should be noted that LG muscle has different compartments that are innervated by two main nerves and numerous sub-branches (41), so stimulation might activate different branches of the muscle causing more variability to the displacement pattern. Furthermore, selective activation of LG might stiffen the connective tissue between SOL and LG, facilitating force transmission (29). Thus, the representation of LG or MG subtendon that we observed within the AT may have been influenced by lateral force transmission at the level of the muscle or tendon. However, this effect was likely minimal since it has been shown that lateral force sharing within the human Achilles tendon is small at low forces (42).

Conclusion

To conclude, Achilles tendon displacement patterns were different in response to selective stimulation of LG compared to MG stimulation or voluntary contraction. Our results suggest that when imaged from a mid-sagittal view, the gastrocnemius subtendons are located in the mid-to-anterior part of the tendon, and that LG is probably located most anteriorly. Previous anatomical studies support these results, but more investigations are needed since results in the literature are inconsistent. The stimulation method could allow for a more individualized approach for investigation of tendon organization, that might help to better understand the complex mechanics and triceps surae subtendon representations within the Achilles tendon. We found no evidence that non-surgical treatment of ATR alters the displacement pattern within the tendon suggesting that non-surgical treatment may preserve the normal subtendon organization. However, differences in displacement amplitude and non-uniformity of the

tendon displacement were present between the limbs in electrically stimulated conditions. These findings suggest an extended toe region of the tendon force-displacement curve after ATR and potential adhesions preventing non-uniform displacements.

Grants

This study was funded by Academy of Finland grant #323168, UNderstanding REStoration of Achilles Tendon function after rupture (UNRESAT), and in part by Academy of Finland grant #332915.

Disclosure

The authors declare that they have no competing interests.

References

1. **Fukashiro S**, **Hay DC**, **Nagano A**. Biomechanical Behavior of Muscle-Tendon Complex during Dynamic Human Movements. *J Appl Biomech* 22: 131–147, 2006. doi: 10.1123/jab.22.2.131.

2. **Roberts TJ**, **Azizi E**. Flexible mechanisms: the diverse roles of biological springs in vertebrate movement. *J Exp Biol* 214: 353–361, 2011.

3. **Ganestam A**, **Kallemose T**, **Troelsen A**, **Barfod KW**. Increasing incidence of acute Achilles tendon rupture and a noticeable decline in surgical treatment from 1994 to 2013. A nationwide registry study of 33,160 patients. *Knee Surg Sports Traumatol Arthrosc* 24: 3730–3737, 2016.

4. **Lantto I**, **Heikkinen J**, **Flinkkilä T**, **Ohtonen P**, **Leppilahti J**. Epidemiology of Achilles tendon ruptures: increasing incidence over a 33-year period. *Scand J Med Sci Sports* 25: e133-138, 2015. doi: 10.1111/sms.12253.

5. **Edama M**, **Kubo M**, **Onishi H**, **Takabayashi T**, **Inai T**, **Yokoyama E**, **Hiroshi W**, **Satoshi N**, **Kageyama I**. The twisted structure of the human A chilles tendon. *Scand J Med Sci Sports* 25: e497–e503, 2015.

6. **Pękala PA**, **Henry BM**, **Ochała A**, **Kopacz P**, **Tatoń G**, **Młyniec A**, **Walocha JA**, **Tomaszewski KA**. The twisted structure of the Achilles tendon unraveled: A detailed quantitative and qualitative anatomical investigation. *Scand J Med Sci Sports* 27: 1705–1715, 2017. doi: 10.1111/sms.12835.

7. **Bojsen-Møller J**, **Magnusson SP**. Heterogeneous Loading of the Human Achilles Tendon In Vivo. *Exerc Sport Sci Rev* 43: 190–197, 2015. doi: 10.1249/JES.0000000000000062.

8. **Beyer R**, **Agergaard A-S**, **Magnusson SP**, **Svensson RB**. Speckle tracking in healthy and surgically repaired human Achilles tendons at different knee angles—A validation using implanted tantalum beads. *Transl Sports Med* 1: 79–88, 2018. doi: 10.1002/tsm2.19.

9. **Slane LC**, **Thelen DG**. Non-uniform displacements within the Achilles tendon observed during passive and eccentric loading. *J Biomech* 47: 2831–2835, 2014.

10. **Thorpe CT**, **Udeze CP**, **Birch HL**, **Clegg PD**, **Screen HR**. Capacity for sliding between tendon fascicles decreases with ageing in injury prone equine tendons: a possible mechanism for age-related tendinopathy. *Eur Cell Mater* 25, 2013.

11. **Clark WH**, **Franz JR**. Do triceps surae muscle dynamics govern non-uniform Achilles tendon deformations? *PeerJ* 6: e5182, 2018. doi: 10.7717/peerj.5182.

12. **Stenroth L**, **Thelen D**, **Franz J**. Biplanar ultrasound investigation of in vivo Achilles tendon displacement non-uniformity. *Transl Sports Med* 2: 73–81, 2019.

13. **Fröberg Å**, **Cissé A-S**, **Larsson M**, **Mårtensson M**, **Peolsson M**, **Movin T**, **Arndt A**. Altered patterns of displacement within the Achilles tendon following surgical repair. *Knee Surg Sports Traumatol Arthrosc* 25: 1857–1865, 2017.

14. **Khair RM**, **Stenroth L**, **Péter A**, **Cronin NJ**, **Reito A**, **Paloneva J**, **Finni T**. Non-uniform displacement within ruptured Achilles tendon during isometric contraction. *Scand J Med Sci Sports* 31: 1069–1077, 2021. doi: https://doi.org/10.1111/sms.13925.

15. **Peng WC**, **Chao YH**, **Fu ASN**, **Fong SSM**, **Rolf C**, **Chiang H**, **Chen S**, **Wang HK**. Muscular Morphomechanical Characteristics After an Achilles Repair. *Foot Ankle Int* 40: 568–577, 2019. doi: 10.1177/1071100718822537.

16. **Svensson RB**, **Couppé C**, **Agergaard A-S**, **Ohrhammar Josefsen C**, **Jensen MH**, **Barfod KW**, **Nybing JD**, **Hansen P**, **Krogsgaard M**, **Magnusson SP**. Persistent functional loss following ruptured Achilles tendon is associated with reduced gastrocnemius muscle fascicle length, elongated gastrocnemius and soleus tendon, and reduced muscle cross-sectional area. *Transl SPORTS Med* 2: 316–324, 2019. doi: 10.1002/tsm2.103.

17. **Hug F**, **Del Vecchio A**, **Avrillon S**, **Farina D**, **Tucker K**. Muscles from the same muscle group do not necessarily share common drive: evidence from the human triceps surae. *J Appl Physiol* 130: 342–354, 2021. doi: 10.1152/japplphysiol.00635.2020.

18. **Masood T**, **Bojsen-Møller J**, **Kalliokoski KK**, **Kirjavainen A**, **Äärimaa V**, **Peter Magnusson S**, **Finni T**. Differential contributions of ankle plantarflexors during submaximal isometric muscle action: A PET and EMG study. *J Electromyogr Kinesiol* 24: 367–374, 2014. doi: 10.1016/j.jelekin.2014.03.002.

19. **Albracht K**, **Arampatzis A**, **Baltzopoulos V**. Assessment of muscle volume and physiological cross-sectional area of the human triceps surae muscle in vivo. *J Biomech* 41: 2211–2218, 2008. doi: 10.1016/j.jbiomech.2008.04.020.

20. **Bojsen-Møller J**, **Schwartz S**, **Kalliokoski KK**, **Finni T**, **Magnusson SP**. Intermuscular force transmission between human plantarflexor muscles in vivo. *J Appl Physiol* 109: 1608–1618, 2010. doi: 10.1152/japplphysiol.01381.2009.

21. **Finni T**, **Cronin NJ**, **Mayfield D**, **Lichtwark GA**, **Cresswell AG**. Effects of muscle activation on shear between human soleus and gastrocnemius muscles. *Scand J Med Sci Sports* 27: 26–34, 2017.

22. **Reito A**, **Logren H-L**, **Ahonen K**, **Nurmi H**, **Paloneva J**. Risk factors for failed nonoperative treatment and rerupture in acute Achilles tendon rupture. *Foot Ankle Int* 39: 694–703, 2018.

23. **Barfod KW**, **Riecke AF**, **Boesen A**, **Hansen P**, **Maier JF**, **Døssing S**, **Troelsen A**. Validation of a novel ultrasound measurement of Achilles tendon length. *Knee Surg Sports Traumatol Arthrosc* 23: 3398–3406, 2015.

24. **Hopkins WG**. Measures of Reliability in Sports Medicine and Science. *Sports Med* 30: 1–15, 2000. doi: 10.2165/00007256-200030010-00001.

25. **Slane LC**, **Thelen DG**. The use of 2D ultrasound elastography for measuring tendon motion and strain. *J Biomech* 47: 750–754, 2014.

26. **Tian M**, **Herbert RD**, **Hoang P**, **Gandevia SC**, **Bilston LE**. Myofascial force transmission between the human soleus and gastrocnemius muscles during passive knee motion. *J Appl Physiol* 113: 517–523, 2012. doi: 10.1152/japplphysiol.00111.2012.

27. **Yin N-H**, **Fromme P**, **McCarthy I**, **Birch HL**. Individual variation in Achilles tendon morphology and geometry changes susceptibility to injury. *eLife* 10: e63204, 2021. doi: 10.7554/eLife.63204.

28. **Bernabei M**, **van Dieën JH**, **Baan GC**, **Maas H**. Significant mechanical interactions at physiological lengths and relative positions of rat plantar flexors. *J Appl Physiol* 118: 427–436, 2015. doi: 10.1152/japplphysiol.00703.2014.

29. **Finni T**, **Bernabei M**, **Baan GC**, **Noort W**, **Tijs C**, **Maas H**. Non-uniform displacement and strain between the soleus and gastrocnemius subtendons of rat Achilles tendon. *Scand J Med Sci Sports* 28: 1009–1017, 2018.

30. **Ekiert M**, **Tomaszewski KA**, **Mlyniec A**. The differences in viscoelastic properties of subtendons result from the anatomical tripartite structure of human Achilles tendon - ex vivo experimental study and modeling. *Acta Biomater* 125: 138–153, 2021. doi: 10.1016/j.actbio.2021.02.041.

31. **Thorpe CT**, **Godinho MS**, **Riley GP**, **Birch HL**, **Clegg PD**, **Screen HR**. The interfascicular matrix enables fascicle sliding and recovery in tendon, and behaves more elastically in energy storing tendons. *J Mech Behav Biomed Mater* 52: 85–94, 2015.

32. **Lehr NL**, **Clark WH**, **Lewek MD**, **Franz JR**. The effects of triceps surae muscle stimulation on localized Achilles subtendon tissue displacements. *J Exp Biol* 224, 2021. doi: 10.1242/jeb.242135.

33. **Francis CA**, **Lenz AL**, **Lenhart RL**, **Thelen DG**. The modulation of forward propulsion, vertical support, and center of pressure by the plantarflexors during human walking. *Gait Posture* 38: 993–997, 2013. doi: 10.1016/j.gaitpost.2013.05.009.

34. **Lenhart RL**, **Francis CA**, **Lenz AL**, **Thelen DG**. Empirical evaluation of gastrocnemius and soleus function during walking. *J Biomech* 47: 2969–2974, 2014. doi: 10.1016/j.jbiomech.2014.07.007.

35. **Clark WH**, **Franz JR**. Age-related changes to triceps surae muscle-subtendon interaction dynamics during walking. *Sci Rep* 11: 21264, 2021. doi: 10.1038/s41598-021-00451-y.

36. **Franz JR**, **Thelen DG**. Imaging and simulation of Achilles tendon dynamics: implications for walking performance in the elderly. *J Biomech* 49: 1403–1410, 2016. doi: 10.1016/j.jbiomech.2016.04.032.

37. **Fröberg Å**, **Cissé A-S**, **Larsson M**, **Mårtensson M**, **Peolsson M**, **Movin T**, **Arndt A**. Altered patterns of displacement within the Achilles tendon following surgical repair. *Knee Surg Sports Traumatol Arthrosc* 25: 1857–1865, 2017. doi: 10.1007/s00167-016-4394-5.

38. **Khair RM**, **Stenroth L**, **Cronin NJ**, **Reito A**, **Paloneva J**, **Finni T**. Muscle-tendon morphomechanical properties of non-surgically treated Achilles tendon 1-year post-rupture. *Clin Biomech* 92: 105568, 2022. doi: 10.1016/j.clinbiomech.2021.105568.

39. **Shin D**, **Finni T**, **Ahn S**, **Hodgson JA**, **Lee H-D**, **Edgerton VR**, **Sinha S**. Effect of chronic unloading and rehabilitation on human Achilles tendon properties: a velocity-encoded phase-contrast MRI study. *J Appl Physiol Bethesda Md 1985* 105: 1179–1186, 2008. doi: 10.1152/japplphysiol.90699.2008.

40. **Svensson RB**, **Slane LC**, **Magnusson SP**, **Bogaerts S**. Ultrasound-based speckle-tracking in tendons: a critical analysis for the technician and the clinician. *J Appl Physiol* 130: 445–456, 2021. doi: 10.1152/japplphysiol.00654.2020.

41. **Segal RL**, **Wolf SL**, **DeCamp MJ**, **Chopp MT**, **English AW**. Anatomical Partitioning of Three Multiarticular Human Muscles. *Cells Tissues Organs* 142: 261–266, 1991. doi: 10.1159/000147199.

42. **Haraldsson BT**, **Aagaard P**, **Qvortrup K**, **Bojsen-Moller J**, **Krogsgaard M**, **Koskinen S**, **Kjaer M**, **Magnusson SP**. Lateral force transmission between human tendon fascicles. *Matrix Biol* 27: 86–95, 2008. doi: 10.1016/j.matbio.2007.09.001.

Achilles MG and LG subtendon representation

Figure captions:

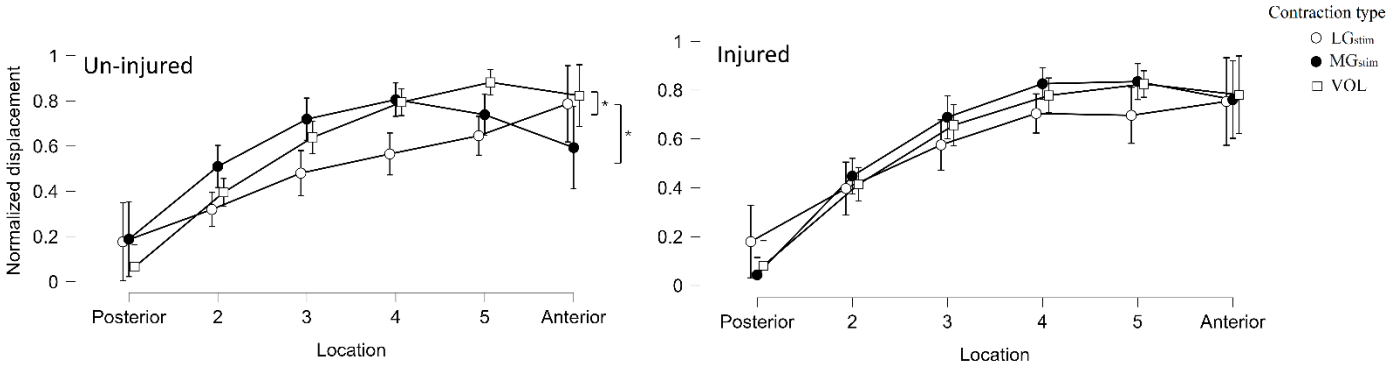

Figure 1. Mean normalized displacement patterns ± SD during voluntary and selective electrically induced contractions of the medial (MG) and lateral (LG) gastrocnemius muscles in the un-injured (left) and injured limb (right). Graphs represent group means Individual patterns in the un-injured limb are shown in Figure 2. * Difference between the contraction types ($p < 0.05$).

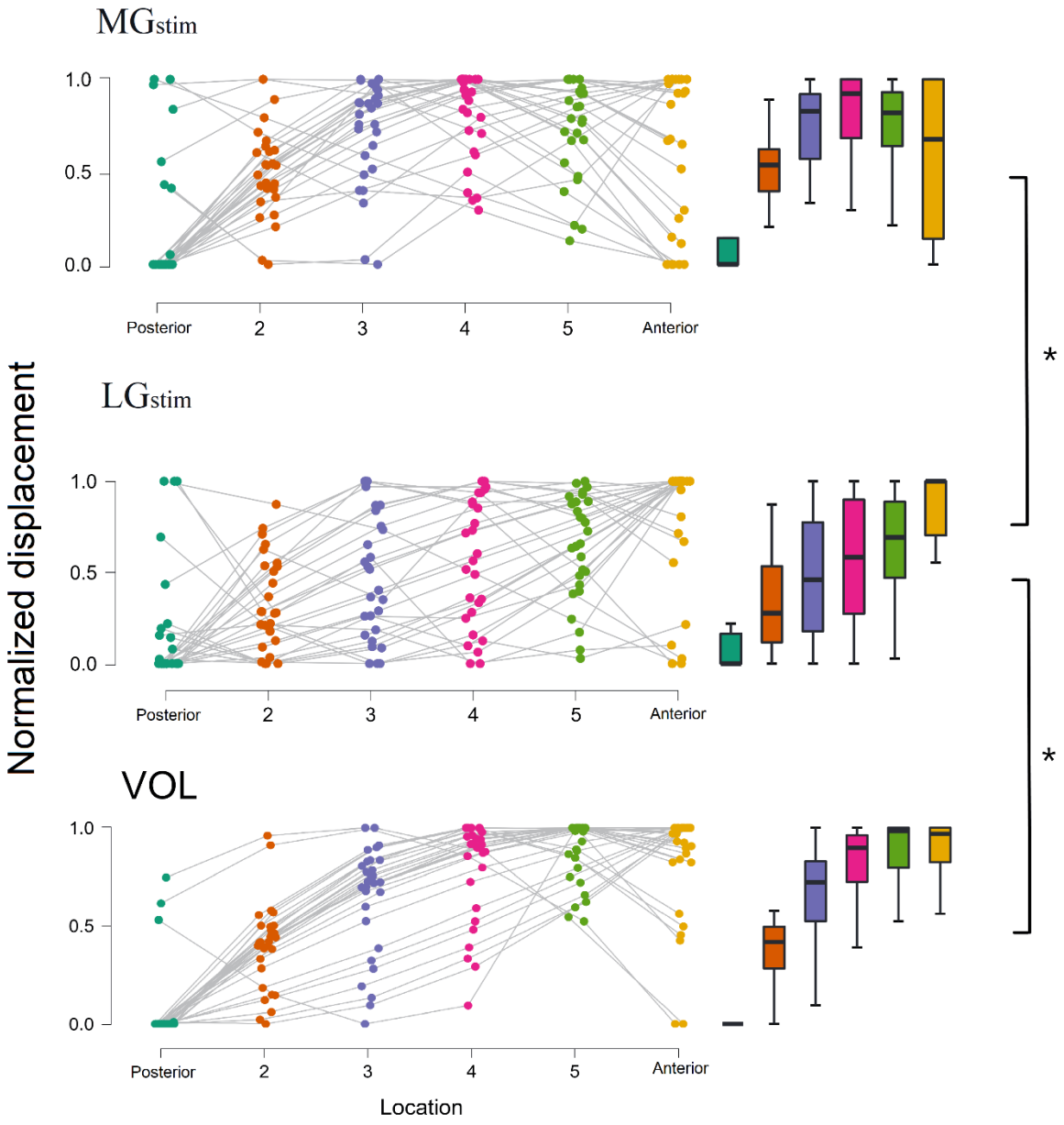

Figure 2. Normalized displacement patterns in the un-injured limb. Left: Raw data points for each participant during voluntary and selective electrical stimulation across the 6 locations of the Achilles tendon. Right: Box plots of means and SD for each location (1-6 respectively). * Difference between the contraction types ($p < 0.05$).

Achilles MG and LG subtendon representation

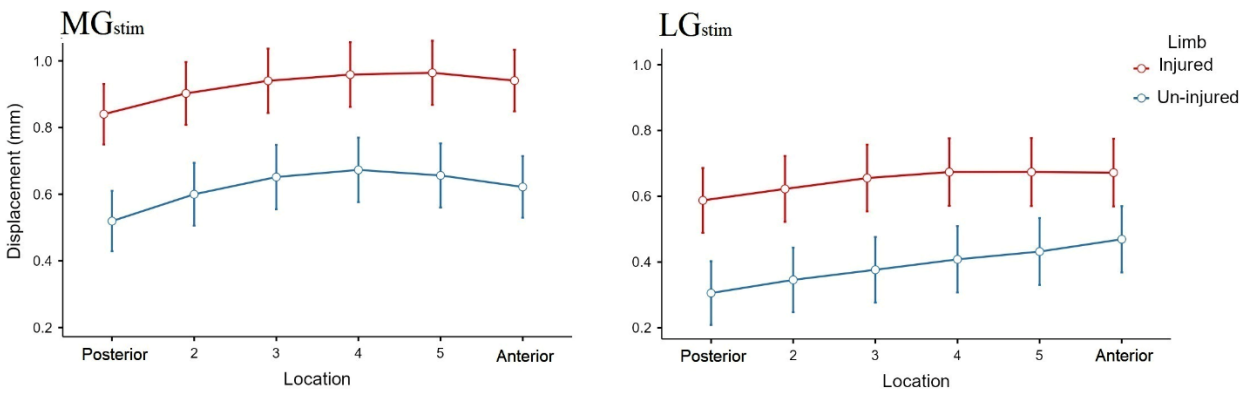

Figure 3. Tendon displacement (mm) of the whole sample during gastrocnemius muscle stimulation at each of the six locations across the tendon width. The values are expressed as mean ± SD.

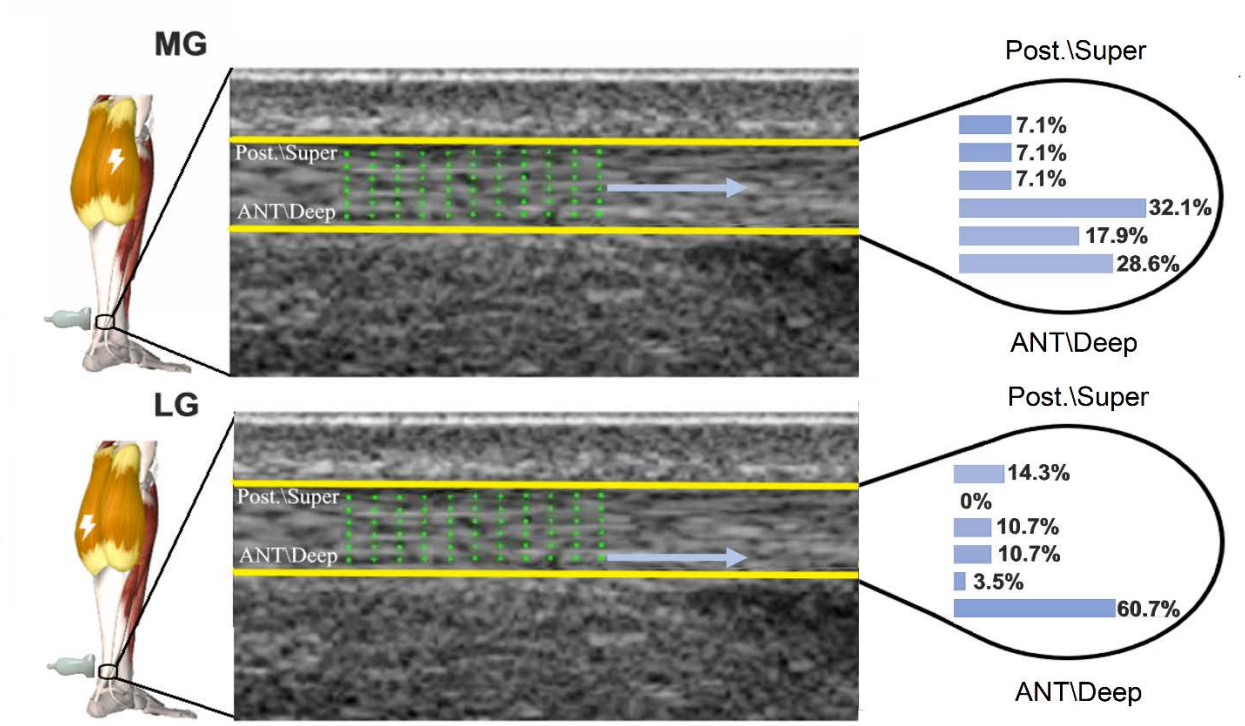

Figure 4. Distribution of peak displacement locations across the tendon in the sagittal view when medial gastrocnemius (MG, upper) or lateral gastrocnemius (LG, lower) was selectively stimulated in the un-injured limb.